Orientational order in high density dipolar hard sphere fluids

Jean-Jacques Weis, Dominique Levesque

May 24, 2006

Orientational order in high density dipolar hard sphere fluids.

J.-J. Weis and D. Levesque*

Laboratoire de Physique Théorique, UMR 8627

Bâtiment 210, Université Paris-Sud, 91405 Orsay Cedex, France

Abstract

Taking advantage of recent estimates, by one of us, of the critical temperature of the isotropic-ferroelectric transition of high density dipolar hard spheres we performed new Monte Carlo simulations in the close vicinity of these estimates and applied histogram reweighting methods to obtain refined values of the critical temperatures from the crossing of the fourth-order cumulant for different system sizes.The ferroelectric line is determined in the density range $\rho^* = 0.80 - 0.95$ and the onset of columnar ordering is located.

I. INTRODUCTION

It is now well established, from simulation and theoretical studies, that at high density, dipolar hard and soft spheres undergo a transition from an orientationally isotropic to an orientationally ordered ferroelectric liquid phase when the temperature is decreased (see refs. 1 and 2 for reviews). Moreover, by further lowering the temperature the system can order into a ferroelectric columnar phase[1,2]. In the past literature the ferroelectric phase has been located by associating, somewhat roughly, the transition with the inflexion point of the order parameter (polarization) computed (generally for rather small system sizes) as a function of density or temperature[3,4]. More precise estimates have been obtained recently by one of us[5] for dipolar hard spheres (DHS) based on the variation of the so-called Binder cumulant[6] involving the fourth and second moments of the polarization (see below) as a function of temperature. The common intersection point of the cumulant curves computed for different system sizes provides, up to finite size effects, an estimate of the critical temperature[6,7]. However, as for the two reduced densities considered[5]($\rho^* = 0.80$ and 0.88) no accurate estimates of the critical temperatures T_c were available from the start a broad range of rather widely spaced temperatures had to be considered thereby limiting the precision of the location of the intersection point. In this paper we describe (Sects. II and III) an attempt to increase the precision of the critical temperature estimates of the isotropic-ferroelectric phase transition by performing calculations in the close vicinity of the previously obtained values for T_c and applying histogram reweighting methods[7] to determine the intersection point of the Binder cumulant curves. Our hope was to obtain, by the same token, compelling estimates of the critical exponents of the transition in order to allow more stringent conclusions concerning the universality class of the long range dipolar interaction as those arrived at in ref. 5. This goal, though, could not be achieved in a completely convincing way, the main reason being that not enough precision could be obtained for the larger system sizes ($N \geq 1000$) within reasonable computer time. In Sect. III we show how the isotropic- ferroelectric transition line can be extended up to the density $\rho^* = 0.95$ and, in Sect. IV, we determine the onset of columnar ordering for the two densities $\rho^* = 0.92$ and 0.95. Discussion and conclusions are given in Sect. V.

II. MODEL AND SIMULATION TECHNIQUES

As in our previous work[5] Monte Carlo (MC) simulations were performed in the canonical (NVT) ensemble using standard Metropolis sampling[8] for system sizes of $N = 256$, 500, 1024 and 2048 dipolar hard spheres interacting by the potential

$$v(\boldsymbol{r}_{ij}, \boldsymbol{s}_i, \boldsymbol{s}_j) = v_{hs}(r_{ij}) + \frac{\mu^2}{r_{ij}^3}\left[\boldsymbol{s}_i \cdot \boldsymbol{s}_j - \frac{3(\boldsymbol{s}_i \cdot \boldsymbol{r}_{ij})(\boldsymbol{s}_j \cdot \boldsymbol{r}_{ij})}{r_{ij}^2}\right] \tag{1}$$

where $v_{hs}(r)$ is a hard sphere potential of diameter σ and v_{dd}, the second term on the r.h.s. of Eq. (1), the dipolar contribution; $\boldsymbol{r}_{ij} = \boldsymbol{r}_j - \boldsymbol{r}_i$ is the vector joining the centers of mass of the particles and $\boldsymbol{s}_i$ a unit vector in the direction of dipole moment i. At the two densities considered $\rho^* = (N/V)\sigma^3 = 0.80$ and 0.88 (V volume) the dimensions of the cubic boxes (with periodic boundary conditions) were $L/\sigma = 6.84, 8.55, 10.86, 13.68$ and $L/\sigma = 6.63, 8.28, 10.52, 13.25$, respectively.

The dipolar energy of the periodic system was evaluated by means of an Ewald sum with conducting boundary conditions[8]. For the parameter α controlling the relative contributions to the Ewald sum of the direct and reciprocal space terms, we adopted the standard value[8] $\alpha L = 5.76$ allowing in the real space term to restrict contributions to the pair interaction truncated at half the box size of the simulation cell. The term in reciprocal space included all lattice vectors $\boldsymbol{G} = 2\pi\boldsymbol{n}/L$, ($\boldsymbol{n} = (n_x, n_y, n_z)$) with $|\boldsymbol{n}|^2 \leq n_{max}^2 = 64$.

A reduced temperature is defined as $T^* = 1/\mu^{*2} = 1/\beta^*$ where $\mu^* = (\mu^2/kT\sigma^3)^{1/2}$ is the reduced dipole moment (k Boltzmann constant, T temperature).

As an efficient cluster update MC algorithm similar to those used for spin systems with short range interactions[7,9] to reduce critical slowing down near the ferroelectric phase transition is not available for the dipolar interaction only single particle moves, translation and rotation of a particle, were implemented.

III. FERROELECTRIC TRANSITION

As stated in the Introduction the critical temperatures are estimated from the Binder cumulant[6,7]

$$U_L(\beta) = 1 - \frac{< m^4 >_L}{3 < m^2 >_L^2} \tag{2}$$

where

$$m = \frac{1}{N}\sqrt{\Big(\sum_{i=1}^{N} \boldsymbol{s}_i\Big)^2} \tag{3}$$

is the polarization (order parameter), m^2 and m^4 the second and fourth moments of the polarization distribution $P(m)$ and $< \cdot >_L$ denotes an ensemble average over a system of characteristic size L.

Up to corrections to scaling the curves $U_L(\beta)$ plotted for different system sizes should intersect at a unique point (β_c, U^*) which provides an estimate of the critical temperature $T_c = 1/\beta_c$ and the universal constant U^* representative of the universality class of the system[7].

As will be shown below the method of histogram reweighting allows to obtain $U_L(\beta)$ as a continuous function of β given the knowledge of the joint distribution of energy and polarization at a few temperatures close to the critical temperature thus facilitating the determination of the intersection point. To this end the histograms $H_i(E)$ and the micro-canonical averages

$$<< m^k >> (E) = \Sigma_M P_{\beta_i}(E, M) m^k / P_{\beta_i}(E) \quad (k = 2, 4) \tag{4}$$

were recorded (for each value of N) at three closely spaced inverse temperatures β_i bracketing the estimates of T_c obtained in ref. 5. Here $P_{\beta_i}(E, M)$ is a two-dimensional histogram of the total energy E and total dipole moment $M = Nm$ and $P_{\beta_i}(E) = \Sigma_M P_{\beta_i}(E, M)$ the energy distribution normalized to unit area at temperature β_i.

Following Ferrenberg and Swendsen[10] an optimized estimate of the density of states $W(E)$ is obtained from a linear combination of the three histograms $H_i(E)$ and minimizing the error on $W(E)$ for each value of E with result

$$W(E) = \frac{\sum_i H_i(E)}{\sum_i \mathcal{N}_i \exp(-\beta_i E - f_i)} \tag{5}$$

where $\mathcal{N}_i$ is the total number of entries in histogram $H_i(E)$.

From the knowledge of $W(E)$ the normalized energy probability function $P_\beta(E)$ follows from

$$P_\beta(E) = W(E) \exp(-\beta E - f) \tag{6}$$

with $\exp(f) = \sum_E W(E) e^{-\beta E}$. The constants f_i in Eq. 5 are determined self-consistently up to a constant from the normalization condition $\sum_E P_\beta(E) = 1$.

The histograms $P_\beta(E)$ or $W(E)$ are computed in the domain of E values from $-2.\mu^{*2}$ to $-1.6\mu^{*2}$. In this range of E the energy step ΔE was taken $\Delta E = 2 \times 10^{-4}$ corresponding to an estimate of $P_\beta(E)$ in the bin $E, \Delta E$ with a statistical error $\sim 1\%$.

The canonical average of any quantity $Q(E)$, in particular $m^k(E)$, can now be calculated as a function of inverse temperature from the normalized energy probability function

$$< Q >= \frac{\sum_E Q(E) P_\beta(E)}{\sum_E P_\beta(E)}. \tag{7}$$

A summary of the various state points, including the number of trial moves, is given in Table I.

The variation of U_L as a function of β^* for the four system sizes is shown in Fig. 1 for $\rho^* = 0.88$ and in Fig. 2 for $\rho^* = 0.80$ together with error bars.

Error bars on $U_L(\beta)$ were estimated in the following way. Average values $< m^2 >$, $< m^4 >$ and $U_L(\beta)$ were calculated by applying the reweighting procedure, Eqs. (5) - (7), to histograms computed for subsets of the total number of entries $\mathcal{N}_i$ of the MC runs at the three temperatures β_i. Over the entire simulation runs generally 20-30 estimates of $Q_L(\beta)$ were obtained allowing to calculate, taking into account the statistical weights, a variance σ^2 and a standard error corresponding to the error bars shown in Figs. 1 and 2. Error bars are largest on the high temperature side of the transition where polarization fluctuations are more important. They are quite substantial, especially in the low density case, for the two largest system sizes for which lower statistics were obtained (cf. Table I).

At density $\rho^* = 0.88$ the curves intersect close to each other at the value $\beta^* \approx 3.812$. A larger spread of intersection points is noticeable for the lower density $\rho^* = 0.80$ ranging (discarding the intersection of the two smallest systems) from $\beta^* = 4.72$ to 4.78. Although different intersection points are expected on ground of finite size effects[6], they should rather be attributed here to statistical error which, as we have seen, is particularly large for the sizes $N = 1024$ and 2048. Safe estimates of the critical temperatures, taking into account the statistical error, are $\beta_c^* = 3.81 \pm 0.01$ at $\rho^* = 0.88$ and $\beta_c^* = 4.75 \pm 0.03$ at $\rho^* = 0.8$.

At these critical temperatures U^* can be estimated, neglecting corrections to scaling, to be $U^* = 0.616 \pm 0.005$ at $\rho^* = 0.88$ and $U^* = 0.625 \pm 0.01$ at $\rho^* = 0.80$. These values are close to that, $U^* = 0.620 - 0.622$ for the simple cubic classical Heisenberg ferromagnet[11–13].

Figure 3 shows a log-log plot of the variation of $< m^2 >$ at $\rho^* = 0.88$ as a function of system size L for different (inverse) temperatures in the vicinity of the critical temperature.

If finite size effects can be neglected $< m^2 >$ should scale with system size as $< m^2 > \propto L^{-2\beta/\nu}$ at the critical temperature, where β and ν are the conventional critical exponents for magnetization[7]. From Fig. 3 it is seen that the "best" linear variation of $\log < m^2 >$ versus $\log L$ occurs near the inverse temperature $\beta^* = 3.79$ with slope $2\beta/\nu \approx 1.05$ close to the value determined for the classical Heisenberg model $\beta/\nu = 0.514$[11,12]. No clear value for the ratio β/ν could, however, been extracted at $\rho^* = 0.8$. In the temperature range $\beta^* = 4.65 - 4.75$, $\log < m^2 >$ varied roughly linearly with $\log L$ with slopes ranging from 1.024-0.80. On one hand, at this lower density, statistical error on $< m^2 >$ and the critical temperature is larger, on the other it is possible that corrections to scaling[15–17] are more important.

Due to the use of the canonical ensemble, which constraints the density of the system, (Fisher) renormalization[14] of the critical exponents β could be expected if the specific heat exponent α is positive. For the dipolar system α is not known; if it were similar to that of the lattice Heisenberg model ($\alpha \approx -0.11$)[11,12] no such renormalization would occur. Corrections to scaling would be either of the Wegner type[15] or arise from the use of the constraint NVT ensemble[17] (especially if α is small) but have been neglected in view of the statistical error on the simulation results.

Determining the critical temperature of the ferroelectric transition by means of the Binder cumulant method is, obviously, a rather arduous task. Therefore, in order to extend the ferroelectric line to higher densities we proceeded in the following more heuristic way. From the polarization curves presented in ref. 5 for $\rho^* = 0.80$ and 0.88 it is observed that, for $N = 1024$, the polarization at the two estimated critical temperatures is very close to $m \sim 0.39 - 0.4$. Assuming that such a criterion remains applicable at somewhat higher densities, we estimated the critical temperature $\beta_c^* \sim 3.42$ ($\mu^* \sim 1.85$) at $\rho^* = 0.92$ and $\beta_c^* \sim 3.17$ ($\mu^* \sim 1.78$) at $\rho^* = 0.95$ (cf. Fig. 4 of the magnetization curves at $\rho^* = 0.92$ and $\rho^* = 0.95$ with $N = 1024$). An alternative procedure is to associate an approximate transition temperature to the value at which $U_L(\beta)$ takes its universal value U^*. Quite satisfactorily, both methods give compatible answers and the results show an almost linear variation of the critical temperatures between $\rho^* = 0.80$ and $\rho^* = 0.95$.

IV. COLUMNAR PHASE.

In earlier work on DHS[18], dipolar soft spheres (DSS)[3] and extended DSS[19] it has been shown that high density dipolar particles can order into a ferroelectric columnar phase at sufficiently low temperature though only qualitative estimates of the transition temperatures were given. The appearance of a columnar phase manifests by a sudden increase of the polarization when the temperature is lowered (cf. Fig. 4). For DHS at densities $\rho^* = 0.92$ and $\rho^* = 0.95$ this increase occurs near $\mu^* \approx 2.8$ ($\beta^* \approx 7.8$) for $\rho^* = 0.92$ and $\mu^* \approx 2.5$ ($\beta^* \approx 6.25$) for $\rho^* = 0.95$. Substantial histeresis precludes more precise estimates of the transition temperatures. Starting from the low temperature columnar phase, columnar ordering is lost at $\mu^* \approx 2.3$ for $\rho^* = 0.92$ and $\mu^* \approx 2.05$ for $\rho^* = 0.95$ which sets lower bound for the ordering temperatures. Histeresis is indicative of a first order transition.

The snapshot of a configuration at $\rho^* = 0.92$ and $\mu^* = 3$ (Fig. 5) shows that columns are aligned parallel to the director and lie in parallel planes. In the plane perpendicular to the director (Fig. 6) they form a square lattice. This seems in contrast with the hexagonal ordering reported for Stockmayer particles with extended dipole moments[19].

V. DISCUSSION.

We have applied histogram reweighting techniques and finite size scaling analysis to the temperature dependence of the Binder cumulant in order to improve the precision of the critical temperature of the ferroelectric transition in the high density DHS fluid. Although the present results are compatible with the earlier ones, a detailed analysis of the error on $U_L(\beta)$ reveals that the error bars for β_c quoted in ref. 5 are underestimated, at least for the low density point $\rho^* = 0.8$. We propose the present estimates of the (inverse) critical temperatures: $\beta_c^* = 3.81 \pm 0.01$ at $\rho^* = 0.88$ and $\beta_c^* = 4.75 \pm 0.03$ at $\rho^* = 0.8$ Error bars are largest on the high temperature side of the transition where fluctuations are more important and increase upon lowering the density. Not surprisingly they also increase with system size as a result of critical slowing down and increase of computer cost for generating particle configurations. In the absence, for the dipolar potential, of an efficient cluster algorithm at least an order of magnitude increase of configurations would be needed for the system sizes $N > 1000$ to derive unambiguous results for the critical exponents. Deriving a

cluster algorithm, as available for lattice or continuum spin systems[9,20], would be a major breakthrough to make progress in the elucidation of the universality class of dipolar fluids.

Despite their limited precision it is nonetheless clear that values of U^* and ν are close to those of the (short range) lattice Heisenberg model. Renormalization-group approaches by Aharony and Fisher[21] and Bruce and Aharony[22] have shown that for a cubic lattice with isotropic exchange (Heisenberg) coupling and dipolar interactions in $d = 4 - \epsilon$ dimensions the critical exponents (except η) differ, to first and second order in ϵ from those of the pure Heisenberg system. They remark, however, that these differences are surprisingly small.

Notwithstanding the failure to give an unambiguous determination of the universality class of the long range dipolar system, a precise location of the ferroelectric line in the density range $\rho^* = 0.8 - 0.95$ is obtained which can serve as a benchmark for theoretical predictions. As summarized in ref. 5 available theories either do not predict a transition at all or severely overestimate the transition temperatures.

Finally, the transition, for DHS, from the isotropic ferroelectric to the columnar ferroelectric phase has been located in the density range $\rho^* = 0.92 - 0.95$. Work on the effect of polidispersity on the ordering in high density DHS is in progress.

Acknowledgments

Computing time was granted by the Institut de Développement et de Ressources en Informatique (IDRIS).

* Electronic address: jean-jacques.weis@th.u-psud.fr; Electronic address: dominique.levesque@th.u-psud.fr

[1] J.-J. Weis and D. Levesque, Adv. Polym. Science **185**, 163 (2005).

[2] C. Holm and J.-J. Weis, Curr. Opin. Colloid Interface Sci. **10**, 133 (2005).

[3] D. Wei and G.N. Patey, Phys. Rev. A **46**, 7783 (1992).

[4] M.J. Stevens and G.S. Grest, Phys. Rev. E **51**, 5976 (1995).

[5] J.-J. Weis, J. Chem. Phys. **123**, 044503 (2005).

[6] K. Binder Z. Phys. B **43**, 119 (1981).

[7] D.P. Landau and K. Binder, *A Guide to Monte Carlo Simulations in Statistical Physics* (Cambridge, UK 2000).

[8] M.P. Allen and D.J. Tildesley, *Computer Simulation of Liquids* (Clarendon, Oxford, 1989).

[9] M.E.J. Newman and G.T. Barkema, *Monte Carlo Methods in Statistical Physics* (Clarendon, Oxford, 1999).

[10] A. M. Ferrenberg and R.H. Swendsen, Phys. Rev. B **63**, 1195 (1989).

[11] C. Holm and W. Janke, Phys. Rev. E **48**, 936 (1993).

[12] K. Chen, A.M. Ferrenberg, and D.P. Landau, Phys. Rev. E **48**, 3249 (1993).

[13] Y. Deng, H.W.J. Blöte, and M.P. Nightingale, Phys. Rev. E **72**, 016126 (2005).

[14] M. E. Fisher, Phys. Rev. **176**, 257 (1968).

[15] C. Domb and M.S. Green (eds.) *Phase Transitions and Critical Phenomena*, Vol 6, (Academic, New York, 1976).

[16] I.M. Mryglod, I.P. Omelyan, and R. Folk, Phys. Rev. Lett. **86**, 3156 (2001).

[17] I.M. Mryglod and R. Folk, Physica A **294**, 351 (2001).

[18] J.J. Weis, D. Levesque, and G.J. Zarragoicoechea, Phys. Rev. Lett. **69**, 913 (1992).

[19] V. Ballenegger and J.-P. Hansen, Mol. Phys. **102**, 599 (2004).

[20] D. Frenkel and B. Smit, *Understanding Molecular Simulation* (Academic, London, 1996).

[21] A. Aharony and M.E. Fisher Phys. Rev. B **8**, 3323 (1973).

[22] A.D. Bruce and A. Aharony Phys. Rev. B **10**, 2078 (1974).

Table caption

Table1: Number of cycles (in units of 10^6) generated for the different system sizes and temperatures. One cycle corresponds to translating and rotating the N particles. U/NkT is the energy devided by the temperature.

Figure captions.

Fig.1: Variation of the Binder cumulant U_L with (inverse) temperature β^* for the four system sizes at $\rho^* = 0.88$. For error bars see text.

Fig.2: Variation of the Binder cumulant U_L with (inverse) temperature β^* for the four system sizes at $\rho^* = 0.80$. For error bars see text.

Fig.3: Log m^2 versus log L at $\rho^* = 0.88$ in the critical region. The slope of the linear least square fit at $\mu^{*2} = 3.79$ is $2\beta/\nu = 1.05$. The value of $2\beta/\nu$ for the lattice Heisenberg model is 1.028[11]. L is in units of σ.

Fig.4: Polarization m as a function of μ^* at (left) $\rho^* = 0.92$ and (right) $\rho^* = 0.95$ for the system size $N = 1024$. The circles (triangles) represent data obtained by increasing (decreasing) μ^*.

Fig.5: Snapshot of a configuration of 1024 DHS particles in the columnar phase at $\rho^* = 0.92$ and $\mu^* = 3$. For clarity the diameter of the particles has been reduced. The dimensions of the simulation cell are in units of σ.

Fig.6: The same configuration as in Fig. 5. Projection on a plane perpendicular to the director. For clarity the diameter of the particles has been reduced.

TABLE I:

ρ^*=0.88				ρ^*=0.80			
T^*	N	nb cycles	U/NkT	T^*	N	nb cycles	U/NkT
	256	175	-6.746		256	60	-8.463
1.94	500	100	-6.748	2.16	500	100	-8.467
	1024	30	-6.743		1024	23	-8.465
	2048	18.5	-6.741		2048	11	-8.465
	256	116	-6.840		256	84	-8.571
1.95	500	90	-6.842	2.17	500	72	-8.576
	1024	30	-6.837		1024	21	-8.571
	2048	7.7	-6.836		2048	7.8	-8.567
	256	144	-6.934		256	50	-8.677
1.96	500	100	-6.938	2.18	500	70	-8.683
	1024	32	-6.935		1024	22	-8.685
	2048	13.7	-6.935		2048	11	-8.682

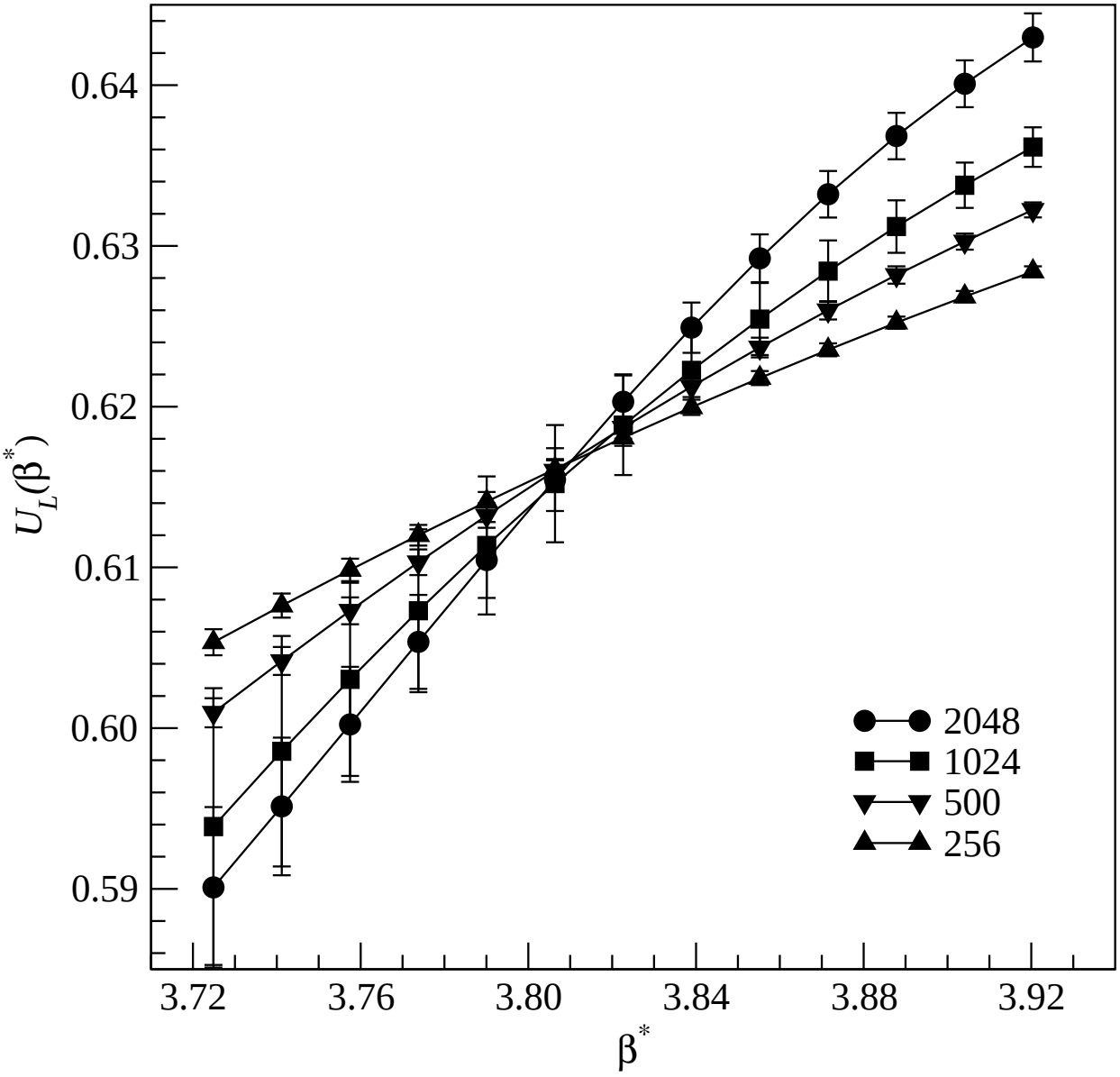
0.64
0.63
0.62
0.61
0.60
0.59
$U_L(\beta^*)$
3.72
3.76
3.80
3.84
3.88
3.92
β^*
2048
1024
500
256

FIG. 1: J.-J. Weis

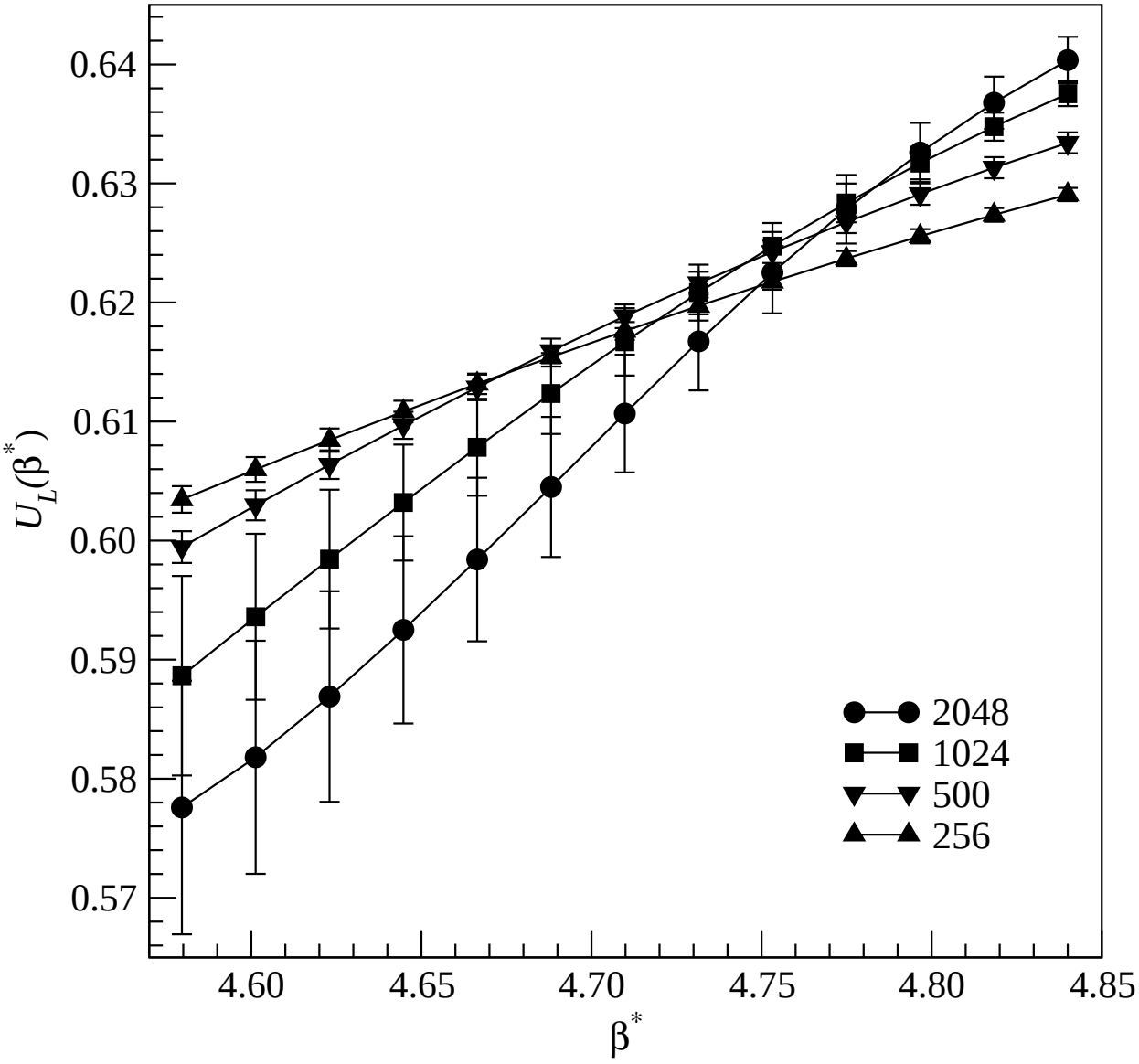
0.64
0.63
0.62
0.61
0.60
0.59
0.58
0.57
$U_L(\beta^*)$
4.60
4.65
4.70
4.75
4.80
4.85
β^*
2048
1024
500
256

FIG. 2: J.-J. Weis

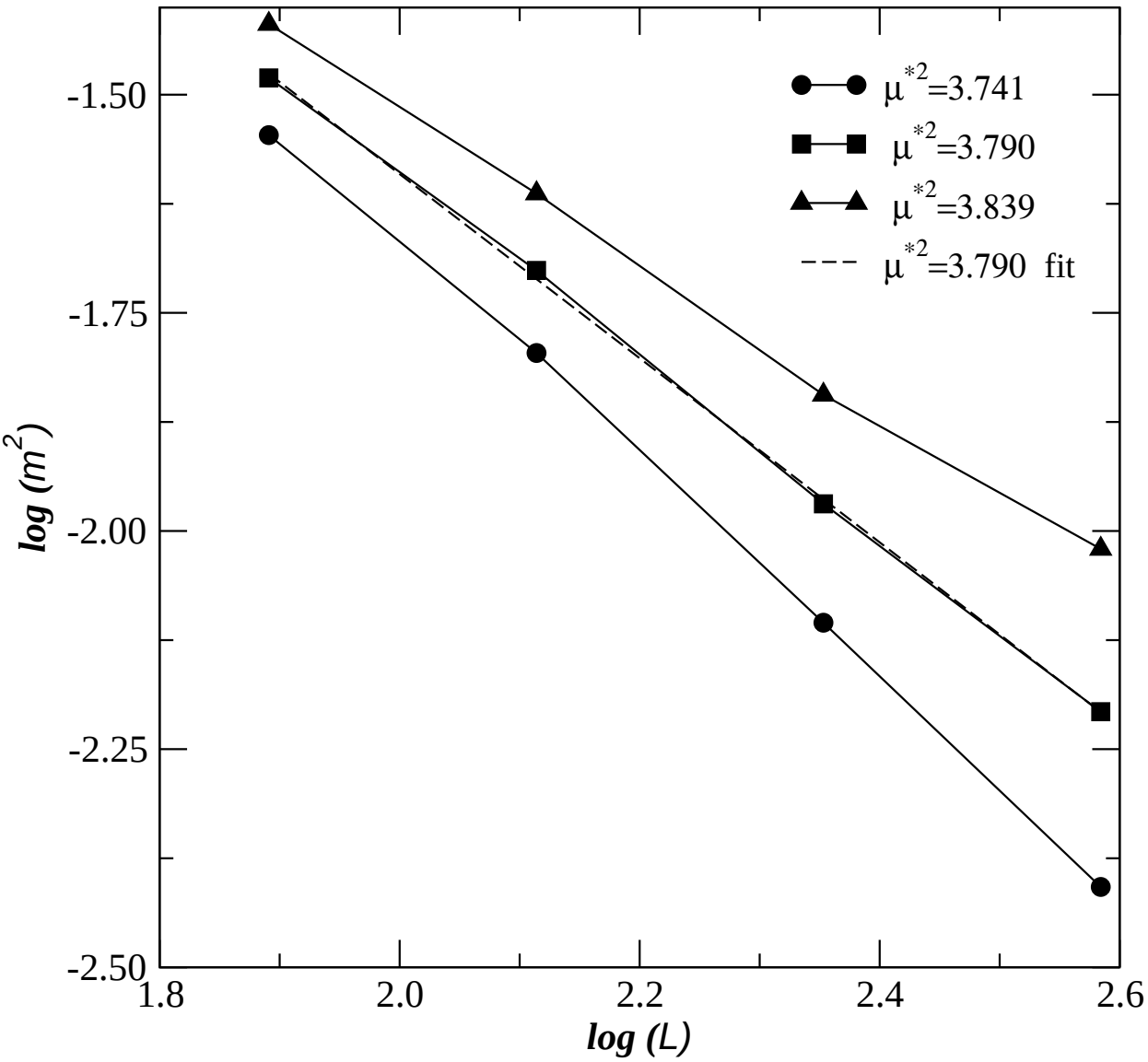
μ*2=3.741
μ*2=3.790
μ*2=3.839
μ*2=3.790 fit
-1.50
-1.75
-2.00
-2.25
-2.50
log (m2)
1.8
2.0
2.2
2.4
2.6
log (L)

FIG. 3: J.-J. Weis

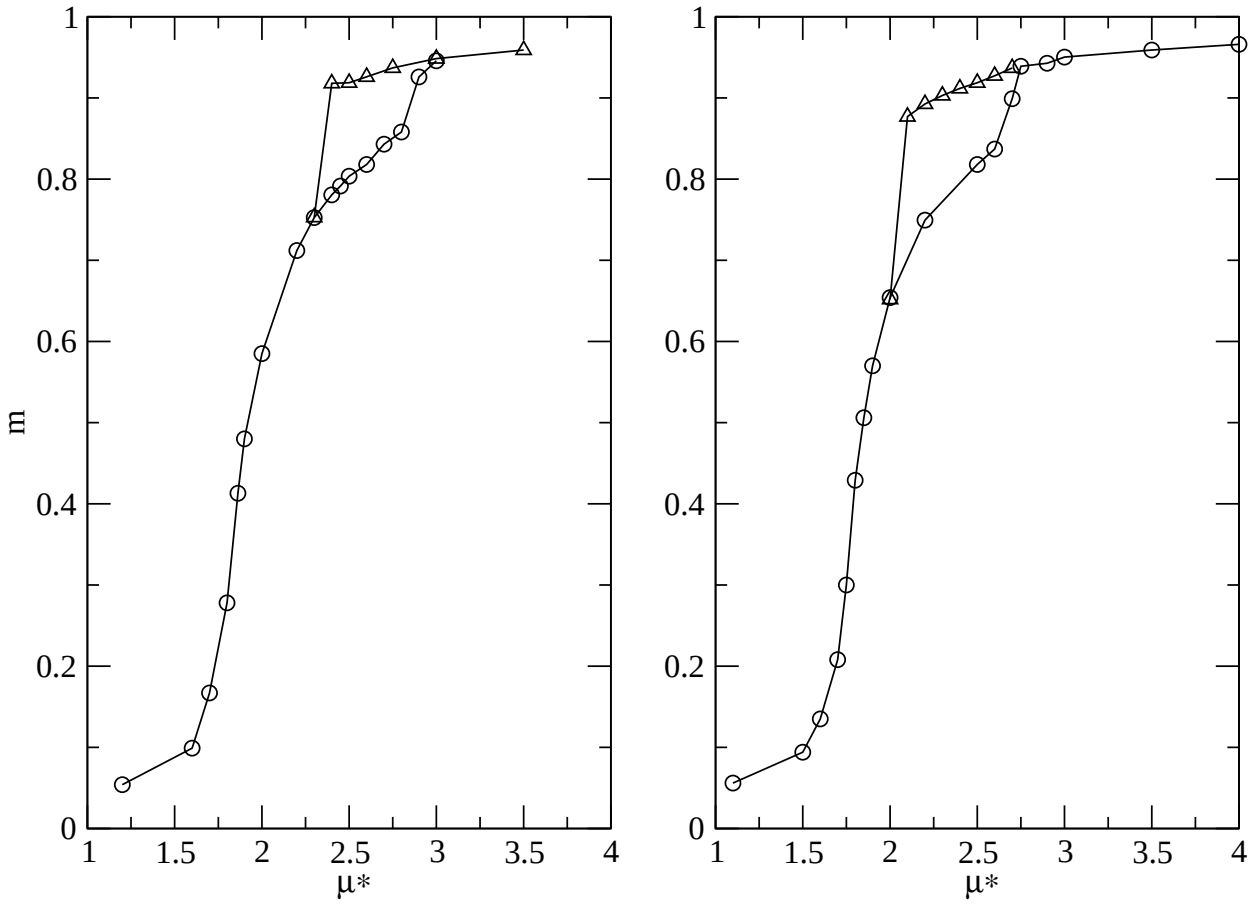

FIG. 4: J.-J. Weis

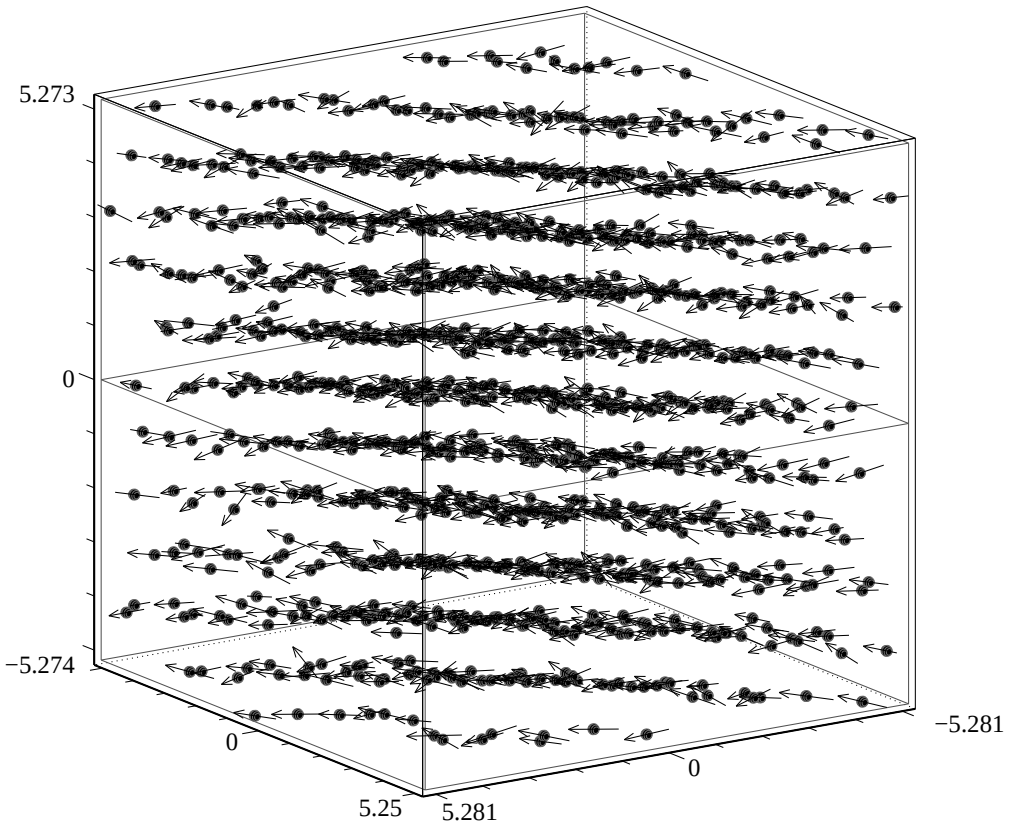

FIG. 5: J.-J. Weis

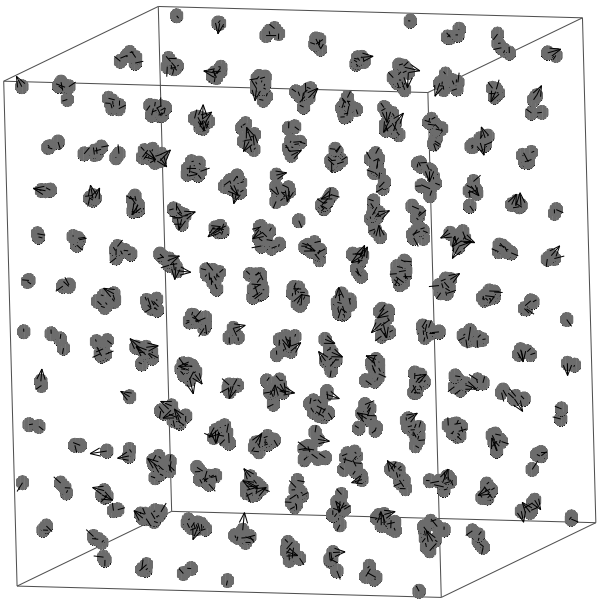

FIG. 6: J.-J. Weis